JACS
JOURNAL OF THE AMERICAN CHEMICAL SOCIETY
Communication
pubs.acs.org/JACS

Microsecond Molecular Simulations Reveal a Transient Proton Pathway in the Calcium Pump

L. Michel Espinoza-Fonseca*,† and G. Lizbeth Ramírez-Salinas‡

†Department of Biochemistry, Molecular Biology and Biophysics, University of Minnesota, Minneapolis, Minnesota 55455, United States

‡Laboratorio de Modelado Molecular y Bioinformática, Escuela Superior de Medicina, Instituto Politécnico Nacional, Mexico City 11340, Mexico

Supporting Information

ABSTRACT: The calcium pump sarcoplasmic reticulum Ca^{2+}-ATPase (SERCA) counter-transports Ca^{2+} and H^+ at the expense of ATP hydrolysis. SERCA uses separate proton and metal ion pathways during active transport to neutralize the highly charged transport site, thus preserving SERCA's structural stability during active Ca^{2+} transport. Although separate metal ion and proton pathways have been identified during slow (millisecond) structural transitions of SERCA, the existence of simultaneous metal and proton pathways during fast (microsecond) structural transitions remains unknown. We have analyzed microsecond-long trajectories of $E1{\cdot}H^+_{771}$, a protonated intermediate of the pump populated during SERCA regulation. We found a transiently established hydrophobic pore in the luminal side of the transmembrane helices 6, 8, and 9. This narrow (0.5−0.6 nm) pore connects the transport sites to the sarcoplasmic reticulum lumen through a chain of water molecules. Protein pK_a calculations of the transport site residues and structural analysis of the water molecules showed that this pore is suitable for proton transport. This transient proton pathway ensures neutralization of the transport sites during the rapid structural transitions associated with regulation of the pump. We conclude that this transient proton pathway plays a central role in optimizing active Ca^{2+} transport by SERCA. Our discovery provides insight into ion-exchange mechanisms through transient hydrophobic pores in P-type ATPases.

The calcium pump sarcoplasmic reticulum Ca^{2+}-ATPase (SERCA) is an intensely studied membrane transporter, truly the biophysical paradigm for active transport and energy transduction[1] in more than 600 homologous P-type ion pumps.[2,3] SERCA clears cytosolic Ca^{2+} in most cells, thus playing a dominant role in Ca^{2+} homeostasis and muscle contractility. In a single catalytic cycle, SERCA undergoes slow (millisecond) structural changes between high (E1) and low (E2) Ca^{2+}-affinity structural states.[4,5] During these structural transitions, the transport sites exchange two Ca^{2+} ions for one or two protons at the expense of ATP hydrolysis.[6,7]

X-ray crystallography and computational studies have suggested that SERCA facilitates Ca^{2+}−H^+ exchange by populating separate metal ion and proton pathways.[8−10] Bublitz et al. used high-resolution crystallographic data to show that SERCA has two cytosolic pathways connecting to the transport sites.[8] These pathways, located at the cytosolic C- and N-terminal transmembrane region of SERCA, were proposed to work in concert during E2−E1 transitions, thus facilitating simultaneous Ca^{2+}−H^+ exchange in the transport sites.[11] The use of separate pathways for Ca^{2+} and H^+ transport is necessary for the structural stability of SERCA because rapid Ca^{2+}−H^+ exchange avoids the highly destabilizing effect of a cluster of negative charges in the transport sites.[12] Indeed, ionization of the transport sites leads to SERCA destabilization[13] and underscores the importance of rapid neutralization of the transport sites upon Ca^{2+} release.[14]

Although separate metal ion and proton pathways have been identified in several biochemical intermediates of the pump during slow (ms) structural transitions, the presence of separate pathways during fast structural transitions (μs) remains unknown. We recently showed that phospholamban (PLB), a 52-residue membrane protein, inhibits SERCA activity by inducing structural changes in the transport sites and promoting protonation of residue E771.[15] These structural changes result in SERCA populating the E1 intermediate state $E1{\cdot}H^+_{771}$.[15] It was proposed that SERCA reactivation occurs when $E1{\cdot}H^+_{771}$ binds a Ca^{2+} in exchange for H^+.[15] This Ca^{2+}−H^+ exchange probably occurs fast, e.g., on the microsecond time scale, because only small structural rearrangements in the transmembrane domain are necessary to populate an active E1 intermediate of the pump.[15] How does Ca^{2+}−H^+ exchange occur during these essential structural transitions of the pump[16] without delaying transport site neutralization? Here we provide a quantitative analysis to show the existence of a transient proton pathway during PLB regulation of SERCA by means of microsecond molecular dynamics (MD) simulations.

We used three recently published microsecond-long MD simulations of the $E1{\cdot}H^+_{771}$-PLB complex[15] to search for potential ion pathways in SERCA. Our analysis included the entire transmembrane domain but excluded the open metal ion pathway previously identified through X-ray crystallography.[8] Analysis of the trajectories revealed the presence of a hydrophobic pore on the luminal side of the transmembrane helices 6, 8, and 9 (Figure 1A). This pore transiently connects the transport sites to the sarcoplasmic reticulum lumen.

Received: April 13, 2015
Published: June 1, 2015

DOI: 10.1021/jacs.5b03814
J. Am. Chem. Soc. 2015, 137, 7055−7058

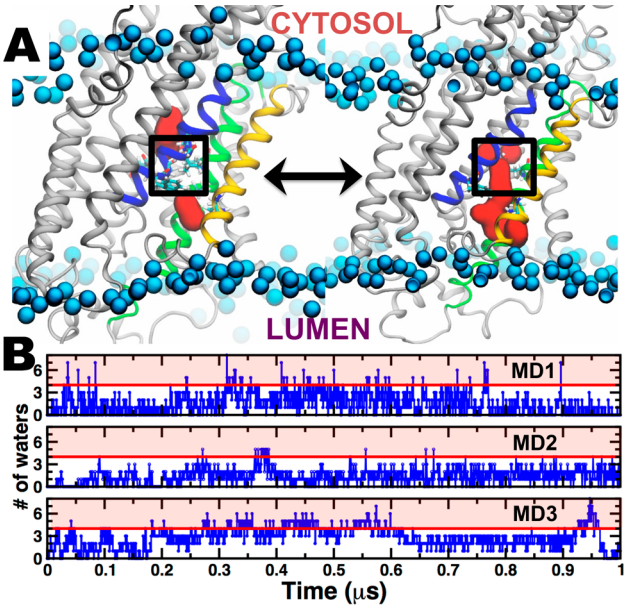

Figure 1. Identification of the hydrophobic pore in the transmembrane domain of SERCA. (A) Location of the pore discovered in MD trajectories of E1·H^+_{771}-PLB.[15] The pore undergoes rapid closed (left) and open (right) transitions. The approximate location of the hydrophobic pore is shown inside the black box; water in the pore is shown as a red surface. SERCA is shown as ribbons, and the transmembrane helices 6, 8, and 9 are shown in blue, green, and yellow, respectively. The cytosolic and luminal sides of the membrane are shown for clarity. (B) Time evolution of the number of water molecules that simultaneously occupy the pore in each MD trajectory of E1·H^+_{771}-PLB. "# of waters" was computed at 1 ns intervals. The points above the red line (shaded area) indicate the presence of an open hydrophobic pore.

Residues T799, E908, V798, V905, W794, and H944 mainly form the pore. This pore is narrow (0.5−0.6 nm in diameter) but sufficiently wide to accommodate water molecules (Figure 1A). We measured the number of water molecules present in the pore at 1 ns intervals to determine whether this pore is formed only transiently (Figure 1B). We found that a minimum of four water molecules must simultaneously occupy the pore to be considered fully open (Figure 1A, right panel). Analysis of the trajectories showed that, although the pore is partially solvated for at least 50% of the simulation time (Figure 1B), an open pore is present only transiently (lifetime between 1 and 10 ns) in E1·H^+_{771}-PLB. The plots shown in Figure 1A also indicate that this pore undergoes open−closed transitions on the nanosecond time scale. For instance, we found at least 20 open−closed transitions over the time interval from 0.36 to 0.39 μs of the trajectory MD2 (Figure 1B).

We compared the structure of the pore between E1·H^+_{771}-PLB and the crystal structure of E1 SERCA bound to Ca^{2+} and an ATP analogue (PDB code 1vfp).[17] We found that, in Ca^{2+}-bound E1 SERCA, residues V798, T799, and V905 form a tightly packed hydrophobic cluster (Figure 2A, left panel). In addition, residues W794 and H944 are also in close contact, thus sealing the pore found in E1·H^+_{771}-PLB (Figure 2A, left). Indeed, distance distribution plots of T799-V905, V798-V905, and W794-H944 showed that inter-residue distances are at least 0.25 nm longer than those of Ca^{2+}-bound SERCA (Figure 2B). This indicates that packing of the hydrophobic cluster V798/T799/V905 is loose in E1·H^+_{771}-PLB, thus facilitating water access to this site. These observations demonstrate that the

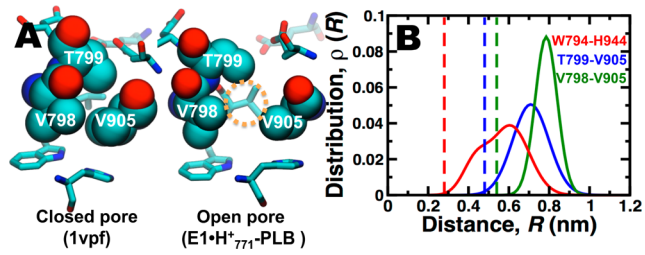

Figure 2. Structure of the hydrophobic pore. (A) Structural arrangement of residues in the closed (left panel) and open (right panel) pores. Residues that participate in the hydrophobic cluster are shown as spheres; other residues are shown as sticks. (B) Inter-residue distances calculated from the MD trajectories of E1·H^+_{771}-PLB. Distance V798-V905 was calculated between C_β atoms; the distance between T799 and V905 was measured using atoms C_γ and C_β, respectively. Finally, we measured the distance between N_ε of W794 and N_δ or N_ε of H944. Inter-residue distances in Ca^{2+}-bound SERCA are shown as dashed lines.

formation of this luminal pore is coupled to the opening of the hydrophobic cluster V798/T799/V905. Although other water-accessible pathways have been identified in E1 SERCA,[8,9] there is no direct experimental evidence supporting the existence of the hydrophobic pore shown in Figure 1A. Hence, a question arises as to whether the presence of this pore is the result of an artifact in the MD simulations. We calculated the distances T799-V905, V798-V905, and W794-H944 using crystal structures of E1 (Table 1) to measure the packing of this

Table 1. Inter-residue Distances in Crystal Structures of E1 SERCA

	distance, R (nm)[a]		
state	T799-V905	V798-V905	W794-H944
E1 (+Ca^{2+})	0.49 ± 0.01	0.55 ± 0.01	0.30 ± 0.01
E1 (−Ca^{2+})[b]	0.64 ± 0.01	0.69 ± 0.01	0.56 ± 0.02

[a]Reported values are mean ± SE. [b]SERCA bound to either SLN or PLB. Ca^{2+}-free state includes two Mg^{2+}-bound structures. Distances were calculated using the atom pairs described in the caption of Figure 2.

pore in different states of E1 SERCA. We used three crystal structures of Ca^{2+}-bound SERCA (PDB codes 1vfp,[17] 1su4,[18] and 4nab[19]) and three structures of inhibited, Ca^{2+}-free SERCA bound to either PLB or sarcolipin (SLN) (PDB codes 3w5a,[20] 4h1w,[21] and 4kyt[22]). We found that hydrophobic cluster V798/T799/V905 is tightly packed in the crystal structures of Ca^{2+}-bound SERCA. W794 and H944 are also in close contact in all crystal structures. Surprisingly, analysis of Ca^{2+}-free SERCA bound to PLB or SLN showed a 0.15 nm increase in the distances T799-V905 and V798-V905, and a 0.26 nm increase in the distance between residues W794 and H944. These distances fall within the distributions calculated for E1·H^+_{771}-PLB (Figure 2B).

We performed four additional 0.5 μs MD simulations starting from two Ca^{2+}-bound structures (1vfp and 1su4) and two Ca^{2+}-free structures bound to SLN (3w5a and 4h1w) to determine the structure of the pore residues at physiological conditions. MD simulations were performed with NAMD[23] in combination with the CHARMM36 force field parameters for protein and lipid[24,25] (methods in Supporting Information). In general, the distance distributions in the hydrophobic cluster of SERCA are in excellent agreement with distances calculated from crystal

DOI: 10.1021/jacs.5b03814
J. Am. Chem. Soc. 2015, 137, 7055−7058

structures (Figure S1). These observations indicate that the MD trajectories correctly capture the structural characteristics of Ca^{2+}-bound and Ca^{2+}-free SERCA. The hydrophobic cluster V798/T799/V905 remains tightly packed in all trajectories of Ca^{2+}-bound SERCA (Figure S1). We found that Ca^{2+}-induced tight packing is sufficient to completely exclude water molecules from this transient pore (Figure S2). On the other hand, Ca^{2+}-free SERCA populates a loosely packed hydrophobic cluster that accommodates more than one water molecule for at least 50% of the simulation time (Figures S1 and S2). This finding is also surprising because the hydrophobic clusters are solvated in Ca^{2+}-free SERCA despite the presence of one or two Mg^{2+} ions in the transport sites.[20,21] This indicates that packing of residues V798, T799, and V905 plays a central role in opening and sealing the pore in E1 SERCA. This quantitative analysis indicates that the presence of the luminal pore is not an artifact of the MD simulations but is an intrinsic structural feature of Ca^{2+}-free, albeit inhibited E1 state of the pump.

We found that the hydrophobic pore is permeable to water molecules but is too narrow to bind metal ions. Indeed, we did not observe the presence of Mg^{2+} or K^+ ions in this pore. What is the functional role of this hydrophobic pore? To answer this question, we analyzed the structural arrangement of water molecules in the open pore. We found a total of ~250 hydrogen-bonded water wires in the hydrophobic pore of E1·H^+_{771}-PLB (Figure 3). The water wires identified in this pore

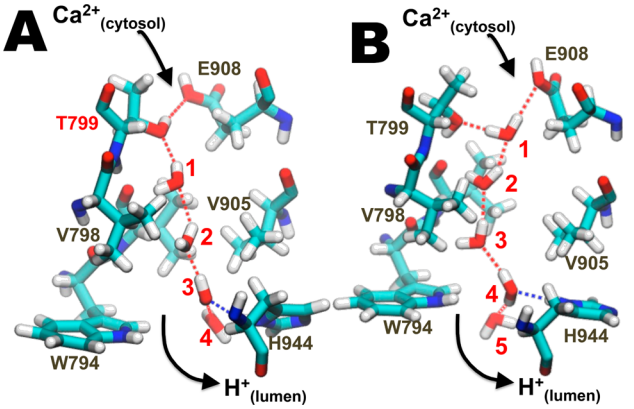

Figure 3. Structure of the water wires: (A) 4-water wire that connects the hydroxyl group of T799 with residue H944. This geometry is populated only in 5% of the water wires found in the simulations. Proton transport proceeds through the triad E908-T799-water. (B) 5-water wire populated in 95% of the water wires identified in the trajectories. This water wire directly connects E908 with the lumen. The arrows indicate the proposed direction of Ca^{2+} binding and H^+ translocation. Residues that form the water pore as well as water molecules are shown as sticks.

fall into two categories: (i) a water wire consisting of four water molecules, formed between the hydroxyl group of residue T799 and the imidazole ring of H944 (Figure 3A), and (ii) a wire consisting of five water molecules, formed between the carboxylic group of E908 and the indole and imidazole rings of W798 and H944, respectively (Figure 3B). The lifetime for each water wire is on the picosecond time scale (Table 2); in general, a water cluster with four members has a much longer lifetime that that of one with five water molecules (Table 2). Despite these differences, both four- and five-membered configuration wires are relatively stable (Table 2). We found

Table 2. Water Wire Lifetimes Calculated in the Trajectories

	water wire lifetime (ps)[a]		
water cluster size	trajectory 1	trajectory 2	trajectory 3
4	168 ± 114	180 ± 111	145 ± 96
5	65 ± 15	45 ± 20	53 ± 17

[a]Calculated from 1 μs MD trajectories reported in ref 15.

that, although both four- and five-membered water wires are present in the trajectories, five-water wires account for ~95% of the water wires found in the pore.

The hydrogen-bond pattern of the water molecules (Figure 3) suggests that this luminal pore can effectively serve as a proton transport pathway during Ca^{2+}–H^+ exchange. It is generally not straightforward to draw firm conclusions regarding proton-transfer pathways based on MD trajectories in the absence of an explicit proton.[26−28] Nevertheless, it is possible to infer whether this pore can be used for proton transport based on a number of assumptions. First, it has been shown that the combination of narrow pores and minimal polar interactions make the Eigen- and Zundel-like ion transition energetically barrierless, thus enhancing Grotthuss shuttling.[29,30] The pore identified in E1·H^+_{771} is very narrow, and at least 60% of the water–protein contacts occur on a hydrophobic surface of SERCA, thus facilitating proton transport. This assumption is supported by a recent study showing that hydrated excess proton can effectively make a hydrophobic space even wetter, thus reducing the electrostatic barrier to proton translocation.[31] Second, we used PROPKA[32,33] to calculate the changes in pK_a of acidic residues E771 and E908 in the presence and absence of water wires, shown in Figure 3. We found that, in the presence of a water wire, the pK_a of E771 remains unchanged (pK_a = 8.5−9.0); however, we found that the pK_a of E908 changes from 7.8 to 7.0 in the presence of a water wire. These protein pK_a calculations indicate that hydration of the hydrophobic pore has a substantial impact on the pK_a of the proton donor, E908, supporting the hypothesis that H^+ shuttling through these water wires initiates in the transport sites. On the basis of these findings, we propose that, upon relief of SERCA inhibition, Ca^{2+} binding to the transport sites and H^+ transfer to the lumen occur simultaneously (Figure 3). The presence of these transient water wires ensures rapid neutralization of the transport sites during the transition E1·H^+_{771} + Ca^{2+} → E1·Ca^{2+} + H^+.[15] The absence of a proton donor (e.g., Glu or Asp) at the luminal side of the pore suggests that proton transfer is primarily unidirectional from transport sites to the lumen. The role of H944 at the luminal side is to stabilize a water molecule at the end of the pathway via a transient hydrogen bond (Figure 3). The stabilizing role of His was demonstrated recently for the influenza A M2 proton channel.[28]

In conclusion, we have identified a transient hydrophobic pore in the transmembrane domain of SERCA that is suitable for proton transfer from the transport sites to the lumen. We propose that transient proton pathway ensures rapid neutralization of the transport sites during the transitions associated with SERCA regulation.[34] We demonstrate that transient ion pathways exist in SERCA and are necessary to optimize active transport during rapid structural transitions of the pump. Although transient proton transfer has been also observed in other transmembrane proteins,[35,36] this study demonstrates for the first time the existence of transient ion pathways in a P-type ATPase. We propose that ion transport through transient pores

DOI: 10.1021/jacs.5b03814
J. Am. Chem. Soc. 2015, 137, 7055−7058

is probably a common theme in the large family of P-type ATPases.

■ ASSOCIATED CONTENT

Supporting Information

Methods, references, and Figures S1 and S2. The Supporting Information is available free of charge on the ACS Publications website at DOI: 10.1021/jacs.5b03814.

■ AUTHOR INFORMATION

Corresponding Author

*espin049@umn.edu.

Notes

The authors declare no competing financial interest.

■ ACKNOWLEDGMENTS

This work was supported by a grant from the American Heart Association (12SDG12060656 to L.M.E.-F.). G.L.R.-S. is supported by a predoctoral fellowship from CONACYT-Mexico. This project made extensive use of the outstanding high-performance computing resources at the Minnesota Supercomputing Institute.

■ REFERENCES

(1) Inesi, G. *Biophys. J.* **1994**, *66*, 554.
(2) Ishii, T.; Hata, F.; Lemas, M. V.; Fambrough, D. M.; Takeyasu, K. *Biochemistry* **1997**, *36*, 442.
(3) Zhang, Z.; Sumbilla, C.; Lewis, D.; Summers, S.; Klein, M. G.; Inesi, G. *J. Biol. Chem.* **1995**, *270*, 16283.
(4) Bublitz, M.; Poulsen, H.; Morth, J. P.; Nissen, P. *Curr. Opin. Struct. Biol.* **2010**, *20*, 431.
(5) Toyoshima, C. *Biochim. Biophys. Acta* **2009**, *1793*, 941.
(6) Yu, X.; Carroll, S.; Rigaud, J. L.; Inesi, G. *Biophys. J.* **1993**, *64*, 1232.
(7) Zafar, S.; Hussain, A.; Liu, Y.; Lewis, D.; Inesi, G. *Arch. Biochem. Biophys.* **2008**, *476*, 87.
(8) Bublitz, M.; Musgaard, M.; Poulsen, H.; Thogersen, L.; Olesen, C.; Schiott, B.; Morth, J. P.; Møller, J. V.; Nissen, P. *J. Biol. Chem.* **2013**, *288*, 10759.
(9) Karjalainen, E. L.; Hauser, K.; Barth, A. *Biochim. Biophys. Acta* **2007**, *1767*, 1310.
(10) Musgaard, M.; Thogersen, L.; Schiott, B.; Tajkhorshid, E. *Biophys. J.* **2012**, *102*, 268.
(11) Yamaguchi, M.; Kanazawa, T. *J. Biol. Chem.* **1985**, *260*, 4896.
(12) Hauser, K.; Barth, A. *Biophys. J.* **2007**, *93*, 3259.
(13) Toyoshima, C.; Cornelius, F. *Curr. Opin. Struct. Biol.* **2013**, *23*, 507.
(14) Obara, K.; Miyashita, N.; Xu, C.; Toyoshima, I.; Sugita, Y.; Inesi, G.; Toyoshima, C. *Proc. Natl. Acad. Sci. U.S.A.* **2005**, *102*, 14489.
(15) Espinoza-Fonseca, L. M.; Autry, J. M.; Ramirez-Salinas, G. L.; Thomas, D. D. *Biophys. J.* **2015**, *108*, 1697.
(16) MacLennan, D. H.; Kranias, E. G. *Nat. Rev. Mol. Cell. Biol.* **2003**, *4*, 566.
(17) Toyoshima, C.; Mizutani, T. *Nature* **2004**, *430*, 529.
(18) Toyoshima, C.; Nakasako, M.; Nomura, H.; Ogawa, H. *Nature* **2000**, *405*, 647.
(19) Clausen, J. D.; Bublitz, M.; Arnou, B.; Montigny, C.; Jaxel, C.; Møller, J. V.; Nissen, P.; Andersen, J. P.; le Maire, M. *EMBO J.* **2013**, *32*, 3231.
(20) Toyoshima, C.; Iwasawa, S.; Ogawa, H.; Hirata, A.; Tsueda, J.; Inesi, G. *Nature* **2013**, *495*, 260.
(21) Winther, A. M.; Bublitz, M.; Karlsen, J. L.; Møller, J. V.; Hansen, J. B.; Nissen, P.; Buch-Pedersen, M. J. *Nature* **2013**, *495*, 265.
(22) Akin, B. L.; Hurley, T. D.; Chen, Z.; Jones, L. R. *J. Biol. Chem.* **2013**, *288*, 30181.
(23) Phillips, J. C.; Braun, R.; Wang, W.; Gumbart, J.; Tajkhorshid, E.; Villa, E.; Chipot, C.; Skeel, R. D.; Kale, L.; Schulten, K. *J. Comput. Chem.* **2005**, *26*, 1781.
(24) Best, R. B.; Zhu, X.; Shim, J.; Lopes, P. E.; Mittal, J.; Feig, M.; Mackerell, A. D., Jr. *J. Chem. Theory Comput.* **2012**, *8*, 3257.
(25) MacKerell, A. D., Jr.; Feig, M.; Brooks, C. L., III. *J. Am. Chem. Soc.* **2004**, *126*, 698.
(26) Wolf, S.; Freier, E.; Cui, Q.; Gerwert, K. *J. Chem. Phys.* **2014**, *141*, 22D524.
(27) Kato, M.; Pisliakov, A. V.; Warshel, A. *Proteins* **2006**, *64*, 829.
(28) Liang, R.; Li, H.; Swanson, J. M.; Voth, G. A. *Proc. Natl. Acad. Sci. U.S.A.* **2014**, *111*, 9396.
(29) Brewer, M. L.; Schmitt, U. W.; Voth, G. A. *Biophys. J.* **2001**, *80*, 1691.
(30) Wu, Y.; Ilan, B.; Voth, G. A. *Biophys. J.* **2007**, *92*, 61.
(31) Peng, Y.; Swanson, J. M.; Kang, S. G.; Zhou, R.; Voth, G. A. *J. Phys. Chem. B* **2014**, DOI: 10.1021/jp5095118.
(32) Olsson, M. H. M.; Sondergaard, C. R.; Rostkowski, M.; Jensen, J. H. *J. Chem. Theory Comput.* **2011**, *7*, 525.
(33) Sondergaard, C. R.; Olsson, M. H. M.; Rostkowski, M.; Jensen, J. H. *J. Chem. Theory Comput.* **2011**, *7*, 2284.
(34) Espinoza-Fonseca, L. M.; Autry, J. M.; Thomas, D. D. *Biochem. Biophys. Res. Commun.* **2015**, DOI: 10.1016/j.bbrc.2015.05.012.
(35) Freier, E.; Wolf, S.; Gerwert, K. *Proc. Natl. Acad. Sci. U.S.A.* **2011**, *108*, 11435.
(36) Wang, D.; Voth, G. A. *Biophys. J.* **2009**, *97*, 121.

DOI: 10.1021/jacs.5b03814
J. Am. Chem. Soc. 2015, 137, 7055−7058